

# Preparation and characterization of multi-walled carbon nanotubes grown on transition metal catalysts

Iwona Pelech\*, Urszula Narkiewicz, Agnieszka Kaczmarek, Anna Jędrzejewska

West Pomeranian University of Technology, Szczecin, Institute of Chemical and Environment Engineering, Pułaskiego 10, 70-322 Szczecin, Poland

\*Corresponding author: e-mail: [ipelech@zut.edu.pl](mailto:ipelech@zut.edu.pl)

Transition metal catalysts (mainly: iron, cobalt and nickel) on various supports are successfully used in a large-scale production of carbon nanotubes (CNTs), but after the synthesis it is necessary to perform very aggressive purification treatments that cause damages of CNTs and are not always effective. In this work a preparation of unsupported catalysts and their application to the multi-walled carbon nanotubes synthesis is presented. Iron, cobalt and bimetallic iron-cobalt catalysts were obtained by co-precipitation of iron and cobalt ions followed by solid state reactions. Although metal particles were not supported on the hard-to-reduce oxides, these catalysts showed nanometric dimensions. The catalysts were used for the growth of multi-walled carbon nanotubes by the chemical vapor deposition method. The syntheses were conducted under ethylene – argon atmosphere at 700°C. The obtained catalysts and carbon materials after the synthesis were characterized using transmission electron microscopy (TEM), X-ray diffraction method (XRD), Raman spectroscopy and thermogravimetric analysis (TG). The effect of the kind of catalyst on the properties of the obtained carbon material has been described.

**Keywords:** catalysts, carbon nanotubes, chemical vapor deposition, X-ray diffraction, thermogravimetry.

## INTRODUCTION

Carbon nanotubes (CNTs) have unique properties, such as: mechanical, chemical or electrical, and for this reason, are of great interest in many areas of science and technology. These properties include an extremely high tensile strength and elastic modulus, high thermal conductivity and the ability (for metallic CNTs) to carry very high current densities<sup>1</sup>. Many methods of the carbon nanotubes synthesis have been developed, among others, in an electric arc discharge<sup>2</sup> or laser sputtering of graphite<sup>3</sup>. One of the most popular methods to obtain carbon nanotubes is the catalytic chemical vapor deposition method<sup>4</sup>, which is characterized by a simple experimental system, easily available reagents and allowing the synthesis of carbon nanotubes in the continuous regime. This technique is based on the hydrocarbons decomposition on the metallic catalysts e.g. iron, nickel, cobalt<sup>5-7</sup>, yttrium or molybdenum<sup>8</sup>. The catalyst particle size is an important factor in CNTs growth. It has been shown, both experimentally and theoretically, that the carbon filaments growth rate increases with decreasing catalyst particle size. Generally, to provide the active catalyst with the desired stability, powder catalysts used for CNTs growth are supported on the hard-to-reduce oxides to minimize the metal particles size. Most often alumina or various kinds of carbon are used as carriers. Specialized supports include silicon dioxide, titanium dioxide or calcium carbonate. Each of the carriers is characterized by both the advantages and the limitations. Calcium oxide shows good performance in CNTs growth in small scale experiments<sup>9-11</sup> and can be easily removed via mild acid treatment<sup>12</sup>. Silica offers high surface areas and good pore size characteristic<sup>13</sup> which allows for a high catalyst loadings (e.g. 60 wt% relative to silica)<sup>14</sup> and hence high yield CNTs growth. However, the large-scale production of high surface area silica (for example, MCM-41 or SBA-15) is time consuming and expensive. Additionally, silica is soluble only in hydrofluoric acid<sup>12</sup>, which is neither comfortable in application nor save for the environment. As in the case of silica, the

properties of alumina can be tuned to create high surface area, mesoporous materials<sup>13</sup>, however the majority of studies using large-scale alumina supported catalysts for CNTs synthesis show the as-produced bulk alumina with promising CNTs growth results<sup>15-17</sup>. Alumina is largely insoluble in acids, yet is readily soluble in alkalies<sup>12</sup>.

Despite the fact that supported catalysts can enhance the effectiveness or decrease the cost, the carbon material after synthesis is additionally contaminated with the support material. In such a case, carbon nanotubes after synthesis require the too aggressive purification treatments, that cause damages of CNTs and in addition – it is not always effective. Therefore synthesizing unsupported powder catalysts with the well-defined and uniform dimensions of the particles is a goal to be pursued.

In the present paper the nanosized iron, cobalt and iron/cobalt based powder catalysts without an inert support were developed in order to prepare carbon nanotubes. The obtained carbon materials have good properties and do not require any removal of supports of catalyst, which is difficult, expensive and time consuming.

## EXPERIMENTAL

### Catalysts preparation

Iron, cobalt and combination of both catalysts were obtained from cobalt (II), and iron (III) nitrates together with a small amount of calcium and aluminum nitrates. The salts were dissolved in distilled water and 20% NH<sub>4</sub>OH was added as a precipitating agent continuously, to obtain a pH of 8. Metal hydroxides were precipitated from the solution and the deposit was washed with water, filtered and dried at 110°C. The next step was the calcination at 500°C for 1h to obtain the precursors of nanocrystalline metals – cobalt and iron oxides with a small amount of structural promoters – CaO and Al<sub>2</sub>O<sub>3</sub>. In the last stage of the preparation the precursors of nanocrystalline metals were reduced under hydrogen atmosphere polythermally at the temperature rising

from 20°C to 600°C with a rate of 10°C/min and next isothermally at 600°C for 90 min in a high-temperature furnace (HST 12/400 Carbolite). The necessary reduction time was determined on the basis of thermogravimetric analysis. For this purpose the catalyst was placed in the platinum basket and heated at a temperature rising from 20°C to 600°C with a rate 10°C/min. The weight changes of the sample were registered. Subsequently the process was continued under hydrogen flow until the constant mass of the sample was reached, which needed 90min. The reduction process was terminated by rapid cooling of the sample under argon atmosphere.

### Carbon nanotubes growth

The synthesis of carbon materials was carried out in a high-temperature furnace (HST 12/400 Carbolite). The samples of the catalyst were placed in a quartz boat inside a ceramic tube (diameter 70 mm, length 120 mm) of the furnace. After the reduction process under hydrogen atmosphere at 600°C the temperature was raised to 700°C and the H<sub>2</sub> flow was turned off. As a carbon source ethylene (20 l/h) was applied. Ar gas (as an inert gas) and C<sub>2</sub>H<sub>4</sub> were introduced together into the chamber. The processes were performed under atmospheric pressure at the temperature 700°C for 60 min.

### Characterization

The morphology of the obtained carbon materials was studied using transmission electron microscopy (high-resolution transmission electron microscope (HRTEM) - FEI Tecnai F20).

The phase composition of the obtained samples was characterized by the X-ray diffraction method. Before the measurement the sample was triturated in an agate mortar and pressed into the ring. The rings were placed in a holder of the diffractometer. The analysis were performed using X'Pert PRO Philips diffractometer using a CuK $\alpha$  radiation.

X-ray fluorescence (XRF) was used for an elemental analysis particularly to investigate the contents of metals in catalysts. The analysis was performed on Epsilon 3 apparatus.

The purity of the carbonaceous material was assessed using Raman spectroscopy. Raman spectroscopy can verify the integrity of MWCNTs because this method is sensitive to variation of structural disorder in carbon nanotubes. The important bands of RS are the D band (1350 cm<sup>-1</sup>), the G band (1580 cm<sup>-1</sup>) and the 2D band (2700 cm<sup>-1</sup>)<sup>18, 19</sup>. Raman measurements were obtained using excitation laser lines 785 nm (1.58 eV) with a Renishaw InVia Raman Microscope spectrometer.

Thermogravimetric analysis was applied to determine the catalyst content in the samples after the CNTs growth and their thermal stability. The thermogravimetric analysis was performed on DTA-Q600 SDT TA Instruments

apparatus with the heating rate of 10°C/min from room temperature to 900°C in air.

## RESULTS AND DISCUSSION

### Catalyst preparation

The chemical composition of the synthesized catalysts after calcination process was analyzed using X-ray fluorescence (XRF). In Table 1 the theoretical and real chemical composition of the prepared catalysts is presented.

Based on the data presented in Table 1 it can be concluded that the real chemical composition of the prepared catalysts was very close to the planned one. In addition, all the catalysts revealed the presence of small amounts of calcium and aluminum oxides, which have been added as structural promoters. The role of these oxides is to prevent the catalyst crystallites against sintering at elevated temperatures in which the synthesis process of carbon nanomaterials is carried out.

The phase composition of the iron, cobalt and iron-cobalt catalysts after calcination was determined using X-ray diffraction method and the diffraction patterns are presented in Figure 1. According to XRD analysis, the catalyst samples contained only the corresponding oxide phases: Co<sub>3</sub>O<sub>4</sub>, Fe<sub>2</sub>O<sub>3</sub> and Fe<sub>3</sub>O<sub>4</sub>. The concentration of the structural promoters was very low and it was determined using XRF analysis (see Table 1). For iron catalyst 2.8 wt.% of Al<sub>2</sub>O<sub>3</sub> and 1.6 wt.% of CaO and for cobalt catalyst 3.5 wt.% of Al<sub>2</sub>O<sub>3</sub> and 0.2 wt.% of CaO was calculated. For both mixed catalyst 2.1wt.% of Al<sub>2</sub>O<sub>3</sub> as well as 2.3 wt.% and 1.8 wt.% of CaO was determined for Fe:Co (65:35) Fe:Co (50:50), respectively. For this reason the peaks corresponding to these phases were not observed on the diffraction patterns, because these values were below detection of the X-ray diffraction method.

On the diffraction pattern corresponding to cobalt catalyst after calcination (Fig. 1Aa) the peaks derived from Co<sub>3</sub>O<sub>4</sub> are visible and on the diffraction pattern corresponding to the iron catalyst after calcination process (Fig. 1Ab) – the peaks derived from Fe<sub>2</sub>O<sub>3</sub> can be identified. For iron-cobalt bimetallic catalysts (Fig. 1B) X-ray diffraction analysis revealed the presence of both Fe<sub>3</sub>O<sub>4</sub> and Co<sub>3</sub>O<sub>4</sub> phases. It was found (see Fig. 1Ba) that the intensity of Co<sub>3</sub>O<sub>4</sub> peaks was lower for the sample Fe-Co (65:35) than for Fe-Co (50:50). This indicates on the smaller cobalt oxide content in the sample Fe-Co (65:35), which is consistent with the theoretical composition of the catalysts and confirms the data obtained using X-ray fluorescence method.

After the calcination, the catalysts were reduced under hydrogen atmosphere. Structural promoters, as compounds resistant to reduction, remained in the oxide state under experimental conditions, whereas transition metal

**Table 1.** Theoretical and real chemical composition of catalysts determined upon XRF analysis

Sample	Chemical composition				
	theoretical	real			
	Fe:Co	Iron (Fe <sub>2</sub> O <sub>3</sub> )	Cobalt (Co <sub>3</sub> O <sub>4</sub> )	Aluminum (Al <sub>2</sub> O <sub>3</sub> )	Calcium (CaO)
		[wt%]			
Co	0:100	<b>0</b>	<b>96.3</b>	3.5	0.2
Fe	100:0	<b>95.6</b>	<b>0</b>	2.8	1.6
Fe:Co (65:35)	65:35	<b>64.2</b>	<b>31.4</b>	2.1	2.3
Fe:Co (50:50)	50:50	<b>51.8</b>	<b>44.3</b>	2.1	1.8

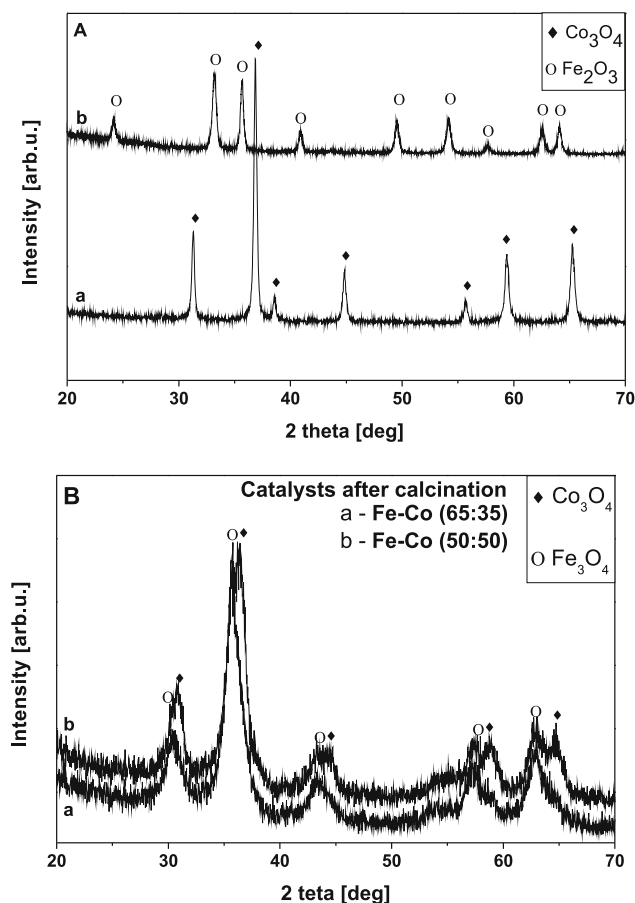


**Figure 1.** Diffraction patterns of catalysts prepared by calcination of cobalt (Fig. 1Aa), iron (Fig. 1Ab), iron-cobalt 65:35 (Fig. 1Ba) and iron-cobalt 50:50 (Fig. 1Bb)

oxides were reduced to metals. Diffraction patterns of the catalysts presented in Figure 2 confirm that after the reduction at 600°C the oxides  $\text{Co}_3\text{O}_4$  and  $\text{Fe}_2\text{O}_3$  were reduced to metallic cobalt or iron in the case of cobalt and iron catalyst (Fig. 2a, 2b) and to iron-cobalt phase in the case of mixed catalysts (Fig. 2c, 2d).

### Carbon nanotubes growth

The morphology of carbon materials after the synthesis obtained on iron, cobalt and iron/cobalt catalyst is presented in Figure 3. The study using Transmission Electron Microscopy revealed that under experimental conditions on all catalysts the carbon material formed filamentous structures (multi walled carbon nanotubes). Material obtained on the cobalt (Fig. 3b) and bimetallic iron-cobalt (Fig. 3c) catalyst was quite homogeneous. The diameters of nanotubes ranged in about 10–30 nm. Bigger catalyst particles encapsulated by graphite layers were also visible, as shown in Fig. 3b. Carbon nanotubes obtained on the iron catalyst (Fig. 3a) were characterized by slightly larger diameters in the range off 20 to 40 nm.

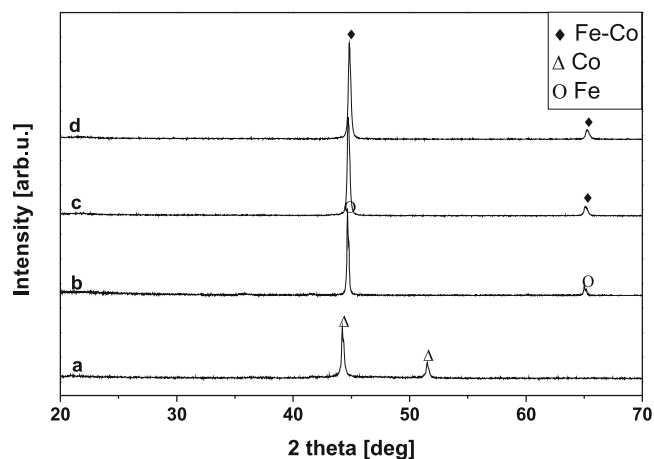


**Figure 2.** Diffraction patterns of cobalt (a), iron (b), iron-cobalt 65:35 (c) and iron-cobalt 50:50 (d) catalysts after reduction process

In this case carbon material was less homogeneous. More encapsulated particles were also observed.

The amounts of carbon deposit obtained during ethylene decomposition on cobalt, iron and two bimetallic iron-cobalt catalysts and the amounts of metal in the individual samples are summarized in Table 2.

It was found that the lowest yield of carbon was obtained on the cobalt catalyst and it was about  $1.8\text{g}_\text{C}/\text{g}_{\text{catalyst}}$  whereas on nanocrystalline iron about  $4.2\text{g}_\text{C}/\text{g}_{\text{catalyst}}$  was achieved. The greatest amounts of carbon were obtained on both iron-cobalt catalysts. More carbon was produced on the sample with higher iron content, on the iron-cobalt catalyst (50:50) about  $6.0\text{g}_\text{C}/\text{g}_{\text{catalyst}}$  but on the iron-cobalt catalyst (65:35) about  $8.7\text{g}_\text{C}/\text{g}_{\text{catalyst}}$  was obtained. The measurements were repeated and the same values of carbon yield on the catalysts were obtained. Probably this effect arises from alloying of Fe and Co in the mixed catalyst, resulting in a better catalytic effect than that of the single elements.

The synthesized materials were characterized using XRD method. In Figure 4 spectra of the cobalt, iron and bimetallic iron-cobalt samples after ethylene decomposition at 700°C are presented.

X-ray diffraction analysis revealed the presence of graphite phase for all the samples after the synthesis on different catalysts. Additionally, on the diffraction pattern of carbon material obtained on cobalt catalyst – the cobalt peaks, which were reduced from cobalt oxide  $\text{Co}_3\text{O}_4$  in hydrogen reduction step were observed (Fig. 4a), whereas on the diffraction pattern of the sample after the carbon nanotubes growth on iron catalyst (Fig. 4b) the peaks corresponding to the cementite phase were present. In the cases of bimetallic iron-cobalt catalysts (Fig. 4c, 4d) the presence of the peaks attributed to Fe-Co phase was revealed and any peaks derived from

**Table 2.** The amount of carbon deposit obtained on cobalt, iron and two bimetallic iron-cobalt catalysts, the quality of the carbon materials expressed as the ratio intensity of peaks IG/ID and the amount of metal in the samples

Sample	Yield of carbon		Ash*	IG/ID**
	$\text{g}_\text{C}/\text{g}_{\text{catalyst}}$		%	–
Co	1.8		33.1	0.72
Fe	4.2		22.2	0.80
Fe:Co (65:35)	8.7		7.2	0.67
Fe:Co (50:50)	6.0		15.0	0.69

\*Determined using thermogravimetric method

\*\*Determined using Raman spectroscopy

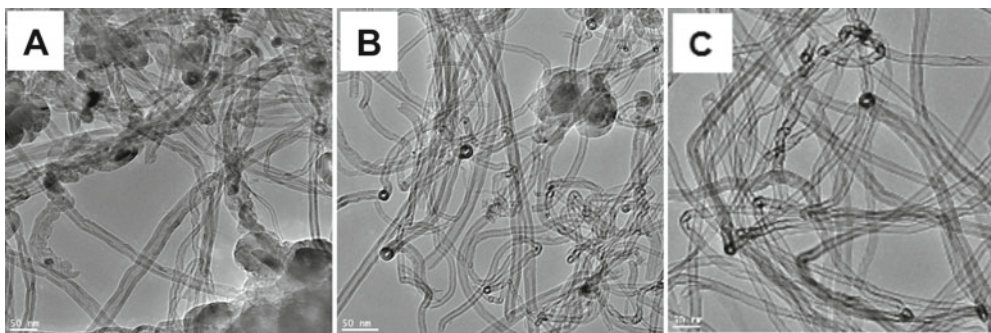


Figure 3. TEM images of the carbon materials obtained on iron (a), cobalt (b) and bimetallic iron/cobalt (c) catalysts

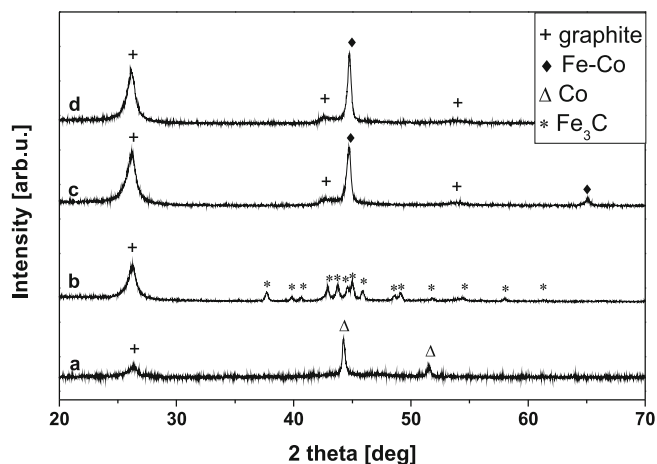


Figure 4. Diffraction patterns of cobalt (a), iron (b), iron-cobalt 65:35 (c) and iron-cobalt 50:50 (d) catalysts after ethylene decomposition

iron carbide were detected. Therefore, one can conclude that in this sample rather Fe-Co phase is present than the separated phases of iron and cobalt, because under the experimental conditions iron particle would react to the cementite<sup>20</sup>.

Based on the thermogravimetric analysis, the amount of metal particles in the samples was determined. The amount of residues remained after the combustion of the samples is presented in Table 2. The highest values of transition metal remained in the samples obtained on cobalt (about 33.1%) and on iron (about 22.0%) catalyst. Smaller amounts of metal were noticed for both bimetallic iron-cobalt catalysts and was about 15.0% for Fe:Co (50:50) and 7.2% for Fe:Co (65:35). It is in good accordance with the efficiency of a given catalyst to produce carbon deposit – the more carbon in the sample after the synthesis, the lower metal content after combustion.

In Figure 5 the weight loss as a function of temperature (A) and the derivative of weight as a function of temperature (B) is presented.

It was found that the mechanism of the combustion of the samples after ethylene decomposition on cobalt (a), iron (b), bimetallic iron-cobalt (65:35) (d) and iron-cobalt (50:50) (c) was similar. Only in the case of iron sample an increase of the mass was observed. Metallic iron is very sensitive to oxidation. In contact with air the metal surface is oxidized and iron react to iron oxide. The lowest initial combustion temperature (about 520°C) characterized a sample obtained on cobalt catalyst (Fig. 6, curve a). Other samples prepared on bimetallic Fe:Co (65:35), Fe:Co (50:50) and iron catalysts, started to burn at higher temperatures: 566°C, 573°C and

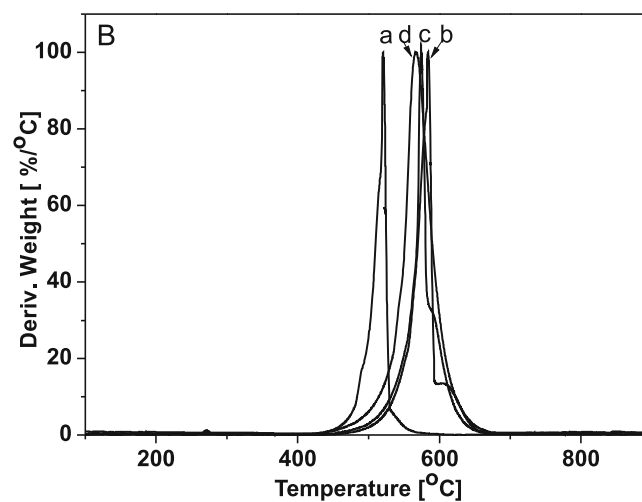
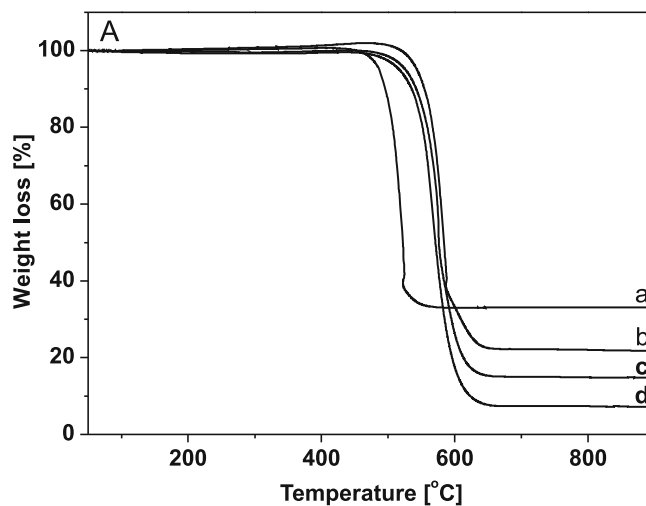


Figure 5. TGA (A) and DTG (B) curves of cobalt (a), iron (b), iron-cobalt 50:50 (c) and iron-cobalt 65:35 (d) samples after ethylene decomposition

583°C, respectively. The lowest combustion temperature of the carbon material prepared on cobalt catalyst may be due to the presence the largest amounts of metal in the sample, in comparison with other materials (see Table 2). This catalyst demonstrated the lowest efficiency towards formation of carbon deposit. During ethylene decomposition from one gram of cobalt catalyst only about 1.8 g of carbon was achieved. Then, one gram of the product contained even 33 wt.% of metal.

The presence of transition metals ions is known to catalyze the gasification of carbon<sup>21</sup>. One theory<sup>21</sup> suggests that metal particles form an intermediate, nonstoichiometric oxide and are then reduced through the oxidation of surrounding carbon particles. In this case, the catalytic

effect of the metal particle would be partially dependent on the thermodynamics of oxidation and would thus vary from one element to another, suggesting a possible reason for the differences between the observed catalytic effects of each metal on the nanotubes. A detailed investigation of the actual mechanism of the catalytic effect is outside of the scope of these experiments. It is important to study this phenomenon and identify the metal, which may be subject to this effect.

An influence of cobalt content in a catalyst on the thermal stability of the carbonaceous material was investigated and described in the paper<sup>22</sup>. The lowest oxidation stability was found for the CNTs obtained from sample containing the most Co (Co3Mn1). The Co-poor sample (Co1Mn3) exhibited the highest oxidation resistance. The difference value between the initial combustion temperature for samples containing the most and least cobalt was 53°C. In another paper<sup>23</sup> comparing the effects of cobalt and iron on the combustion of carbonaceous material obtained on pure metals cobalt and iron, cobaltocene  $\text{Co}(\text{C}_5\text{H}_5)_2$  and ferrocene  $\text{Fe}(\text{C}_5\text{H}_5)_2$  and a cobalt chloride was described. For each catalyst TG curves were shifted towards lower temperatures.

The same effect was clearly observed for our material obtained by ethylene decomposition on cobalt catalyst. In the case of the sample obtained on iron catalyst a higher initial combustion temperature was noticed than for the material obtained on cobalt catalyst, what is consistent with the results presented in the previously discussed work<sup>23</sup>.

For the carbon material obtained on both bimetallic catalysts a lower thermal stability was observed than for the sample prepared on the iron catalyst, despite the lower amount of metal particles per one gram of carbon deposit. After a combustion in air atmosphere 22%, 15% and 7.2% of metal oxide particles was presented in the material obtained on the iron, iron-cobalt (50:50) and iron-cobalt (65:35), respectively. So, it seems that in the case of cobalt, the catalytic effect is more visible than in the case of iron. Therefore an addition of cobalt to the sample, like in the case of both bimetallic catalysts, caused a reduction of thermal stability of the carbon material.

The purity of the carbonaceous materials synthesized on the different catalysts was determined using Raman spectroscopy and the Raman spectra are presented in Figure 6. In all cases typical spectra characteristic for multi walled carbon nanotubes were received<sup>24, 25</sup>.

Raman spectroscopy can verify the integrity of MWCNTs because this method is sensitive to variations of structural disorder in carbon nanotubes. The important bands of Raman spectrum are the D band ( $1350\text{ cm}^{-1}$ ), the G band ( $1580\text{ cm}^{-1}$ ) and the 2D band ( $2700\text{ cm}^{-1}$ )<sup>18, 19</sup>. The D band is attributed to the breathing vibrations of  $\text{sp}^3$  hybridized carbon atoms of defects or amorphous carbon in MWCNTs, while the G band is caused by the tangential vibrations of  $\text{sp}^2$ -hybridized carbon atoms of graphite layers. The intensity ratio of the D and G band peaks (ID/IG) is often used to assess the purity of carbon nanotubes<sup>18, 19</sup>. The 2D band is caused by the two-phonon, second-order scattering around the K point of the Brillouin zone and is an indicator of long-range order in a sample. It is well known to be sensitive to the increasing defect density of carbon nanotubes<sup>19</sup>. The presence of the D and G bands

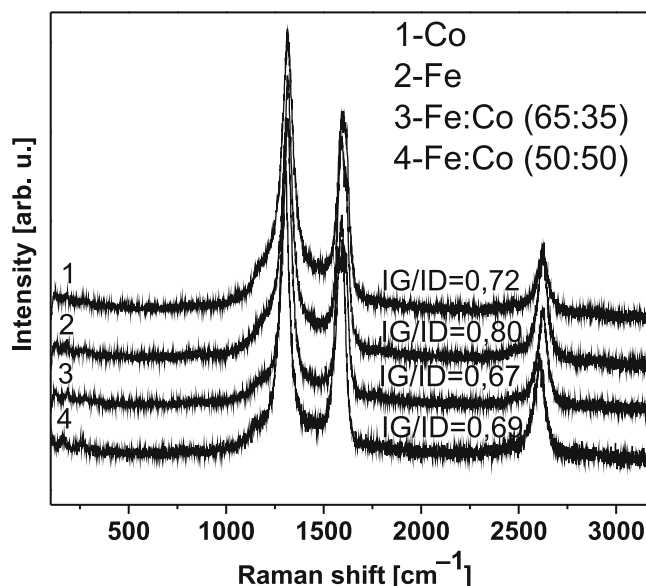


Figure 6. Raman spectra of the carbon materials obtained on the different catalysts

can explain that the graphitic structure of all MWCNTs is conserved. For our samples the ratio of intensity peak IG/ID equaled in order of: 0.80, 0.72, 0.69, 0.67 for the carbon material obtained on iron, cobalt, iron-cobalt (50:50) and iron-cobalt (65:35) catalysts, respectively. It can indicate that the carbon material prepared on iron catalyst had a lowest amount of structural defects in the graphite structure of MWCNTs<sup>24-26</sup>.

The presence of defects can be studied by not only using the Raman spectroscopy but also thermogravimetric method. It has been reported<sup>27</sup> that the stability of carbon samples during the combustion in the air atmosphere is associated with the crystallinity degree of carbon nanotubes and it is also attributed to the presence of defects at the ends of the nanotubes. Generally, higher thermal stability of the samples suggests higher structural order and a lower number of defects, as edges, vacancies, kinks and steps. Comparing the results obtained using the Raman spectroscopy and thermogravimetric analysis we cannot completely confirm this relationship for the samples obtained in this work.

For our samples the highest ratio of peak intensities IG/ID = 0.80 (theoretically the lowest number of defects) was achieved for the carbon material obtained on the iron catalyst. This material also burnt at the highest temperature. The lowest ratio of peak intensities IG/ID equaled about 0.68 (theoretically the highest number of defects) was assigned to the carbon material obtained on the mixed catalysts. These materials should burn at the lowest temperature. In contrast to this, the material obtained on the cobalt catalyst burnt at the lowest temperature (Fig. 5). The obtained results confirm that not only the structural defects have the influence on the thermal stability of the samples obtained by decomposition of ethylene on metal catalysts but the thermal stability of the carbon material also depends on the kind of the metal used as the catalyst.

## CONCLUSION

In this work a nanosized iron, cobalt and iron/cobalt based powder catalysts without inert support were deve-

loped, characterized and applied for carbon nanotubes preparation. The obtained carbon materials have good structural properties (low degree of defects) and, contrary to supported catalysts, do not require a removal of supports of catalyst, which is difficult, expensive and time consuming.

The highest quantity of carbon deposit was obtained on the bimetallic catalysts, the lowest on the cobalt catalyst. The purity of carbon material determined using the Raman spectroscopy was quite similar for all materials. The lowest thermal stability during combustion under air atmosphere exhibited the sample obtained on the cobalt catalyst. It indicates that not only the structural defects have a significant influence on the thermal stability of the samples obtained by decomposition of ethylene on metal catalysts, but the thermal stability also depends on the kind of the metal used as the catalyst.

#### ACKNOWLEDGEMENTS

This work was supported by project: LIDER/25/58/l-3/11/NCBR/2012 financed by The National Centre for Research and Development.

The authors are grateful Dr Zofia Lendzion-Bieluń for the studies using X-ray fluorescence method.

#### LITERATURE CITED

- Hong, S. & Myung, S. (2007). Nanotube electronics: a flexible approach to mobility. *Nat. Nanotechnology* 2, 207–208. DOI: 10.1038/nnano.2007.89.
- Journet, C., Maser, W.K., Bernier, P., Loiseau, A., Lamy de la Chapelle, M., Lefrant, S., Deniard, P., Lee, R., & Fischer, J.E. (1997). Large-scale production of single-walled carbon nanotubes by the electric-arc technique. *Nature* 388, 756–758.
- Guo, T., Nikolaev, P., Thess, A., Colbert, D.T. & Smalley, R.E. (1995). Catalytic growth of single-walled nanotubes by laser vaporization. *Chem. Phys. Lett.* 243, 49–54. DOI: 10.1016/0009-2614(95)00825-O.
- Qiu, J., An, Y., Zhao, Z., Li, Y. & Zhou, Y. (2004). Catalytic synthesis of single-walled carbon nanotubes from coal gas by chemical vapor deposition method. *Fuel Process. Technol.* 85, 913–920. DOI: 10.1016/j.fuproc.2003.11.033.
- Sengupta, J. & Chacko, J. (2009). Growth temperature dependence of partially Fe filled MWCNT using chemical vapor deposition. *J. Cryst. Growth* 311, 4692–4697. DOI: 10.1016/j.jcrysgro.2009.09.029.
- Deck, Ch.P. & Vecchio, K. (2006). Prediction of carbon nanotube growth success by the analysis of carbon–catalyst binary phase diagrams. *Carbon* 44, 267–275. DOI: 10.1016/j.carbon.2005.07.023.
- Journet, C., Picher, M. & Jourdain, V. (2012). Carbon nanotube synthesis: from large-scale production to atom-by-atom growth. *Nanotechnology* 13, 1–19. DOI: 10.1088/0957-4484/23/14/142001.
- Esconjauregui, S., Whelan, C.M. & Maex, K. (2009). The reasons why metals catalyze the nucleation and growth of carbon nanotubes and other carbon nanomorphologies. *Carbon* 47, 659–669. DOI: 10.1016/j.carbon.2008.10.047.
- Liu, B.C., Yu, B. & Zhang, M.X. (2005). Catalytic CVD synthesis of double-walled carbon nanotubes with a narrow distribution of diameters over Fe-Co/MgO catalyst. *Chem. Phys. Lett.* 407, 232–235. DOI: 10.1016/j.cplett.2005.03.093.
- MacKenzie, K., Dunens, O., Harris, A.T. (2009). A review of carbon nanotube purification by microwave assisted acid digestion. *Sep. Purif. Technol.* 66, 209–222. DOI: 10.1016/j.seppur.2009.01.017.
- Mauron, P., Emmenegger, Ch., Sudan, P., Wenger, P., Rentsch, S. & Züttel, A. (2003). Fluidised-bed CVD synthesis of carbon nanotubes on Fe<sub>2</sub>O<sub>3</sub>/MgO. *Diamond Relat. Mater.* 12, 780–785. DOI: 10.1016/S0925-9635(02)00337-0.
- Weast, R.C. (1980). *CRC Handbook of Chemistry and Physics* (60th ed.). CRC Press, Boca Raton, Florida, USA.
- Schwarz, J.A., Contescu, C. & Contescu, A. (1995). Methods for preparation of catalytic materials. *Chem. Rev.* 95, 477–510. DOI: 10.1021/cr00035a002.
- Li, Y.L., Kinloch, I.A., Shaffer, M.S.P., Geng, J., Johnson, B., Windle, A.H. (2004). Synthesis of single-walled carbon nanotubes by a fluidized-bed method. *Chem. Phys. Lett.* 384, 98–102. DOI: 10.1016/j.cplett.2003.11.070.
- See, C.H. & Harris, A.T. (2007). On the development of fluidized bed chemical vapour deposition for large-scale carbon nanotube synthesis: Influence of synthesis temperature. *Aust. J. Chem.* 60, 541–546. DOI: 10.1071/CH06398.
- Chai, S.P., Zein, S.H.S. & Mohamed, A.R. (2007). The effect of reduction temperature on Co-Mo/Al<sub>2</sub>O<sub>3</sub> catalysts for carbon nanotubes formation. *Appl. Catal. A: General* 326, 173–179. DOI: 10.1016/j.apcata.2007.04.020.
- Dikonimos Makris, Th., Giorgi, L., Giorgi, R., Lisi, N. & Salernitano, E. (2005). CNT growth on alumina supported nickel catalyst by thermal CVD. *Diamond Relat. Mater.* 14, 815–819. DOI: 10.1016/j.diamond.2004.11.001.
- Edwards, E.R., Antunes, E.F., Botelho, E.C., Baldan, M.R. & Corat, E.J. (2011). Evaluation of residual iron in carbon nanotubes purified by acid treatments. *Appl. Surf. Sci.* 258, 641–648. DOI: 10.1016/j.apsusc.2011.07.032.
- Lehman, J.H., Terrones, M., Mansfield, E., Hurst, K.E. & Meunier, V. (2011). Evaluating the characteristics of multi-walled carbon nanotubes. *Carbon* 49, 2581–2602. DOI: 10.1016/j.carbon.2011.03.028.
- Narkiewicz, U., Podsiadły, M., Jędrzejewski, R. & Petech, I. (2010). Catalytic decomposition of hydrocarbons on cobalt, nickel and iron catalysts to obtain carbon nanomaterials. *Appl. Catal. A: General* 384, 27–35. DOI: 10.1016/j.apcata.2010.05.050.
- Thomas, J.M. (1965). *Microscopic Studies of Graphite Oxidation. Chemistry and Physics of Carbon*; Walker, P.L., Jr., Ed.; Marcel Dekker: New York, 1, 121–202.
- Becker, M. J., Xia, W., Tessonnier, J.P., Blume, R., Yao, L., Schlögl R. & Muhler M. (2011). Optimizing the synthesis of cobalt-based catalysts for the selective growth of multiwalled carbon nanotubes under industrially relevant conditions. *Carbon* 49, 5253–5264. DOI: 10.1016/j.carbon.2011.07.043.
- McKee, G.S.B. & Vecchio, K.S. (2006). Thermogravimetric analysis of synthesis variation effects on CVD generated multiwalled carbon nanotubes. *J. Phys. Chem. B* 110, 1179–1186. DOI: 10.1021/jp054265h.
- Koos, A.A., Dillon, F., Obraztsova, E.A., Crossley, A. & Grobert, N. (2010). Comparison of structural changes in nitrogen and boron-doped multi-walled carbon nanotubes. *Carbon* 48, 3033–3041. DOI: 10.1016/j.carbon.2010.04.026.
- Irani, F., Jannesari, A. & Bastani, S. (2013). Effect of fluorination of multiwalled carbon nanotubes (MWCNTs) on the surface properties of fouling-release silicone/MWCNTs coatings. *Prog. Org. Coat.* 76, 375–383. DOI: 10.1016/j.porgcoat.2012.10.023].
- Ko, F-H., Lee, C-Y., Ko, C-J. & Chu, T-C. (2005). Purification of multi-walled carbon nanotubes through microwave heating of nitric acid in a closed vessel. *Carbon* 43, 727–733. DOI: 10.1016/j.carbon.2004.10.042].
- Bom, D., Andrews, R., Jacques, D., Anthony, J., Chen, B., Meier, M.S. & Selegue, J.P. (2002). Thermogravimetric analysis of the oxidation of multiwalled carbon nanotubes: evidence for the role of defect sites in carbon nanotubes chemistry. *Nano Lett.* 2, 615–619. DOI: 10.1021/nl020297u.